in vivo *37*: 163-172 (2023)
doi:10.21873/invivo.13065

Systemic Administration of Lipopolysaccharide from *Porphyromonas gingivalis* Decreases Neprilysin Expression in the Mouse Hippocampus

TETSURO MORIKAWA[1], OSAMU UEHARA[2], DURGA PAUDEL[3], KOKI YOSHIDA[1], FUMIYA HARADA[4], DAICHI HIRAKI[5], JUN SATO[1], HIROFUMI MATSUOKA[2], YASUHIRO KURAMITSU[3], MAKOTO MICHIKAWA[6] and YOSHIHIRO ABIKO[1]

[1]*Division of Oral Medicine and Pathology, Department of Human Biology and Pathophysiology, School of Dentistry, Health Sciences University of Hokkaido, Ishikari-Tobetsu, Japan;*
[2]*Division of Disease Control and Molecular Epidemiology, Department of Oral Growth and Development, School of Dentistry, Health Sciences University of Hokkaido, Ishikari-Tobetsu, Japan;*
[3]*Advanced Research Promotion Center, Health Sciences University of Hokkaido, Ishikari-Tobetsu, Japan;*
[4]*Division of Oral and Maxillofacial Surgery, Department of Human Biology and Pathophysiology, School of Dentistry, Health Sciences University of Hokkaido, Ishikari-Tobetsu, Japan;*
[5]*Division of Reconstructive Surgery for Oral and Maxillofacial Region, Department of Human Biology and Pathophysiology, School of Dentistry, Health Sciences University of Hokkaido, Ishikari-Tobetsu, Japan;*
[6]*Department of Biochemistry, Graduate School of Medical Sciences, Nagoya City University, Nagoya, Japan*

Abstract. *Background/Aim: Alzheimer's disease is the most common type of neurodegenerative disorder in elderly individuals worldwide. Increasing evidence suggests that periodontal diseases are involved in the pathogenesis of Alzheimer's disease, and an association between periodontitis and amyloid-β deposition in elderly individuals has been demonstrated. The aim of the present study was to examine the effects of systemic administration of Porphyromonas gingivalis-derived lipopolysaccharide (PG-LPS) on neprilysin expression in the hippocampus of adult and senescence-accelerated mice. Materials and Methods: PG-LPS diluted in saline was intraperitoneally administered to male C57BL/6J and senescence-accelerated mouse prone 8 (SAMP8) mice at a dose of 5 mg/kg every 3 days for 3 months. Both C57BL/6J and SAMP8 mice administered saline without PG-LPS comprised the control group. The mRNA expression levels of neprilysin and interleukin (IL)-10 were evaluated using the quantitative reverse transcriptase-polymerase chain reaction. The protein levels of neprilysin were assessed using western blotting. Sections of the brain tissues were immunohistochemically stained. Results: The serum IL-10 concentration significantly increased in both mouse strains after stimulation with PG-LPS. Neprilysin expression at both mRNA and protein levels was significantly lower in the SAMP8 PG-LPS group than those in the SAMP8 control group; however, they did not differ in PG-LPS-treated or non-treated C57BL/6J mice. Additionally, the immunofluorescence intensity of neprilysin in the CA3 region of the hippocampus in PG-LPS-treated SAMP8 mice was significantly lower than that in control SAMP8 mice. Conclusion: Porphyromonas gingivalis may reduce the expression of neprilysin in elderly individuals and thus increase amyloid-β deposition.*

Correspondence to: Yoshihiro Abiko, Division of Oral Medicine and Pathology, Department of Human Biology and Pathophysiology School of Dentistry, Health Sciences University of Hokkaido 1757 Kanazawa, Ishikari-Tobetsu, Hokkaido, 061-0293, Japan. Tel: +81 133231390, Fax: +81 133231390, e-mail: yoshi-ab@hoku-iryo-u.ac.jp

Key Words: Alzheimer's Disease, neprilysin, periodontitis, *Porphyromonas gingivalis*, hippocampus.

Alzheimer's disease is the most common type of neurodegenerative disorder in elderly individuals worldwide. Pathologically, it is characterised by considerable neuronal loss in the brain with two typical protein deposits, amyloid plaques, and neurofibrillary tangles, extracellularly and intracellularly, respectively (1). Although Alzheimer's disease has been extensively studied, effective prevention and treatment strategies have not yet been established.

Table I. *Primers used in quantitative reverse transcriptase polymerase chain reaction.*

Gene	Forward (5'-3')	Reverse (5'-3')	NCBI reference sequence
GAPDH	AGAACATCATCCCTGCATCC	CACATTGGGGGTAGGAACAC	NM_001289726.1
IL-10	CCAAGCCTTATCGGAAATGA	TCTCACCCAGGGAATTCAAA	NM_010548.2
TNF-α	CAGGCGGTGCCTATGTCTC	CGATCACCCCGAAGTTCAGTAG	NM_013693.3
IL-6	CCGGAGAGGAGACTTCACAG	TCCACGATTTCCCAGAGAAC	NM_031168.2
IL-1β	GAGTGTGGATCCCAAGCAAT	TACCAGTTGGGGAACTCTGC	NM_008361.4
Neprilysin	AATGCTCCAAAGCCAAAGAA	CGATCATTGTCACCGCTATG	NM_001289462.1
C1QTNF5	GAACCTGAGGACCAGGTGTG	GGAGCTGTGCCAGTCAGAAT	NM_145613.4
GPNMB	GGCGTACAAGCCAATAGGAA	GGATCCTTCTCCTGGTCTCC	NM_053110.4
OLFML3	AGAGGCTGCGTTTGTCATCT	AGTACCACTGGCATCGAAGG	NM_133859.2
SLIT2	AAACCTCTTGGCCAATCCTT	TTTTTGGCATCGAGGATTTC	NM_001291227.2
SMOC1	AAGAGCATAGAGGCCGATGA	CCTGAACCATGTCTGTGGTG	NM_001146217.1
SPON1	CGTGAGGGATACACGGAGTT	TGAAGTAGGAGGGAGGAGCA	NM_145584.2

The two hypotheses that explain the pathogenesis of Alzheimer's disease are the amyloid cascade hypothesis and hyperphosphorylated tau protein hypothesis (2). The amyloid cascade hypothesis attributes amyloid-β peptide deposition in the brain parenchyma for the development of Alzheimer's disease. Amyloid-β peptide, formed from the proteolytic processing of amyloid-β precursor protein, causes senile plaques that lead to neurofibrillary degeneration and neuronal loss, resulting in Alzheimer's disease (3). Amyloid-β is typically eliminated from the brain *via* a clearance mechanism; however, overproduction of amyloid-β or a defect in the clearance mechanism increases amyloid-β deposition in the brain (2, 4). Enzymes that degrade amyloid-β deposits include neprilysin, insulin-degrading enzyme, and endothelin-converting enzyme (4). Neprilysin (also known as neutral endopeptidase, cluster of differentiation 10, and common acute lymphoblastic leukaemia antigen) is a type II integral plasma membrane protein that is widely distributed in various organs. An active catalytic site of neprilysin faces the extracellular space. It acts as an ectoenzyme to proteolytically cleave various substrates extracellularly. As neprilysin has been found to cleave amyloid b peptides, it has been widely evaluated as a potential therapeutic agent (5). In rat models, a correlation has been observed between the amyloid-b peptide level in the brain and neprilysin (6). These reports suggest that neprilysin is a promising therapeutic target for Alzheimer's disease (7).

Increasing evidence suggests that periodontal diseases are involved in the pathogenesis of Alzheimer's disease, and an association between periodontitis and amyloid-β deposition in elderly individuals has been demonstrated (8, 9). In aged rats, infection with *Porphyromonas gingivalis*, the pathogen causing periodontitis, induces up-regulated expression of inflammatory cytokines such as tumour necrosis factor α, interleukin (IL)-6, and IL-1β, accompanied by memory disturbance (10). Inflammation caused by *P. gingivalis* infection may increase amyloid-β deposition (11) and may induce cerebral inflow of amyloid-b *via* the receptor of advanced glycation end products (12). Although periodontal diseases are known to enhance amyloid-b deposition, it remains unclear whether enzymes that degrade amyloid-b are altered by periodontal diseases. In our previous study, we developed a mouse model that is not affected by *P. gingivalis*-derived lipopolysaccharide (PG-LPS)-induced acute inflammation to evaluate the effects of LPS on the kidney and pancreas (13, 14). In the present study, we aimed to examine the effects of systemic administration of PG-LPS on neprilysin expression in the hippocampus of adult and senescence-accelerated mice.

Materials and Methods

Animals. Male C57BL/6J (6-8 weeks old) and senescence-accelerated mouse prone 8 (SAMP8) mice (6-8 weeks old) were purchased from Sankyo Labo Service Corporation (Tokyo, Japan). The mice were reared under specific pathogen-free conditions in clear cages under a 12-h light/dark cycle with *ad libitum* access to standard rodent feed and water. The experimental protocol was approved by the Animal Experimental Committee and Ethics Committee of the Health Sciences University of Hokkaido (approval number 073). The experiments complied with the Animal Research: Reporting of In Vivo Experiments (ARRIVE) guidelines. The mice were randomly divided into two groups: control group and PG-LPS group (n=5 of each mouse strain for each analysis including polymerase chain reaction (PCR), western blotting, and histological analysis). The sample size was determined based on our previous study and the law of diminishing return using the resource equation method (14, 15). PG-LPS (ATCC 33277; Wako, Osaka, Japan) diluted in saline was intraperitoneally administered to the mice in the PG-LPS group (5 mg/kg) every 3 days (84 h) for 3 months, as previously reported (13, 14). The control group mice were administered the same volume of saline without PG-LPS. The mice were euthanised using intraperitoneal injection of pentobarbital (100 mg/kg body weight). The brain, hippocampal tissue, and blood were collected from each mouse.

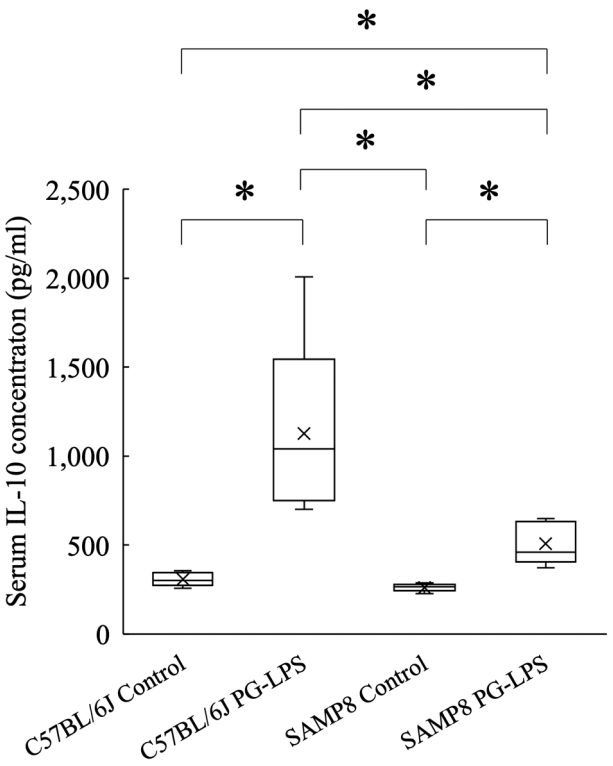

Figure 1. *Comparison of serum IL-10 concentration between C57BL/6J and SAMP8 mice using enzyme-linked immunosorbent assay. SAMP8 mice showed significantly lower serum IL-10 concentration than C57BL/6J mice. *p<0.05. (The bar in the box plot represents median and the cross represents mean; Kruskal-Wallis test followed by Holm method, n=5).*

Enzyme-linked immunosorbent assay. Blood samples were collected from the mouse hearts 1 h after each PG-LPS or saline administration. The samples were incubated for 15 min at room temperature and then centrifuged for 20 min at 100×*g* to separate the serum. Serum IL-10 concentration was measured using an IL-10 mouse uncoated enzyme-linked immunosorbent assay kit (Thermo Fisher Scientific, Waltham, MA, USA).

Quantitative reverse transcriptase PCR. RNA was extracted from the hippocampal tissues using the RNeasy Mini kit (Qiagen, Hilden, Germany). The extracted RNA was reverse transcribed into cDNA using the ReverTra Ace qPCR RT Master Mix kit (Toyobo, Osaka, Japan). The mRNA expression level was evaluated using quantitative PCR performed using the LightCycler Nano instrument (Roche Diagnostics, Basel, Switzerland) and KAPA SYBR FAST qPCR Mix (Kapa Biosystems, Cape Town, South Africa). Table I illustrates the primer sequences used in this study. PCR was conducted in two-step amplification that included initial denaturation at 95˚C for 10 min, 40 cycles of denaturation at 95˚C for 10 s, and annealing at 60˚C for 30 s. The relative mRNA expression level was calculated using the $2^{-\Delta\Delta Cq}$ method (16), with *GAPDH* as the internal control.

Western blotting. Protein was extracted from the hippocampal tissue using the WSE-7420 EzRIPA Lysis kit (ATTO Technology, Amherst, NY, USA), and 15 μg of protein was used for western blotting. Pre-cast 5%-20% gradient polyacrylamide gels (e-PAGEL; ATTO Technology) were used for sodium dodecyl sulphate-polyacrylamide gel electrophoresis. The separated proteins were transferred onto polyvinylidene fluoride membranes (ATTO Technology), which were then blocked with Tris-buffered saline containing 5% skim milk at room temperature for 1 h followed by incubation at 4˚C overnight with the following primary antibodies: monoclonal rabbit anti-neprilysin antibody (1:1,000; Abcam, Cambridge, UK) diluted in Can Get Signal Solution 1 (Toyobo) and monoclonal mouse anti-GAPDH antibody (1:10,000; ProteinTech Group, Rosemont, IL, USA) diluted in Tris-buffered saline containing 5% skim milk. The membranes were washed with Tris-buffered saline containing 0.05% Tween-20 three times and incubated with secondary antibodies, namely, horseradish peroxidase-conjugated goat anti-rabbit immunoglobulin G (1:10,000; ProteinTech Group) diluted in Can Get Signal Solution 2 (Toyobo) and horseradish peroxidase-conjugated goat anti-mouse immunoglobulin G (1:2,000; ProteinTech Group) at room temperature for 1 h. Immunoreactive protein bands were visualised *via* enhanced chemiluminescence (Clarity Western ECL substrate; Bio-Rad, Hercules, CA, USA) and WSE-6100 LuminoGraph I (ATTO Technology). Band intensities were quantified using ImageJ imaging software (v.1.53a; National Institutes of Health, Bethesda, MD, USA).

Histological observation.

Haematoxylin–eosin staining. The hippocampal tissues isolated from the PG-LPS-treated and control C57BL/6J and SAMP8 mice were fixed in 10% neutral buffered formalin solution. The tissues were embedded in paraffin and sectioned (5.0-μm thick). The sections were subjected to haematoxylin–eosin staining and observed using the Olympus BX50 microscope (Olympus, Tokyo, Japan) for morphological analysis.

Immunofluorescence staining. The brain tissues from SAMP8 mice were subjected to immunofluorescence staining. After deparaffinisation, the sections were inactivated in 10 mM citrate buffer (pH 6.0) for 5 min using a pressure cooker, and endogenous peroxidase was inactivated by incubation in 3.0% hydrogen peroxide methanol for 5 min. To block non-specific immunoreactivity, the sections were treated using an avidin and biotin blocking kit (Vector Laboratories, Burlingame, CA, USA) and the Tyramide Signal Amplification kit (TSA Biotin System; NEN Life Science Products, Boston, MA, USA). The sections were then incubated with anti-neprilysin (56C6; 1:100 dilution; Abcam) antibody diluted with Tris-buffered saline (0.1 M Tris-HCl, 0.15 M NaCl, pH 7.5) as the primary antibody at 4˚C overnight. After three washes in TNT buffer (0.1 M Tris-HCl, 0.15 M NaCl, and 0.05% Tween-20, pH 7.5) for 5 min, the sections were incubated with biotin-conjugated goat anti-mouse immunoglobulin G (H&L; 1:3,000 dilution; SouthernBiotech, Birmingham, AL, USA) for 1 h and streptavidin-horseradish peroxidase (1:100 dilution, supplied with the TSA Biotin System kit) for 30 min; thereafter, the sections were washed with TNT buffer three times, for 5 min each time. The sections were then incubated with biotinyl tyramide amplification reagent (1:50 dilution; TSA Biotin) at room temperature for 10 min. Alexa Fluor 488-conjugated streptavidin (1:500 dilution; NEN Life Science Products) was added, and the sections were incubated for 1 h and subsequently

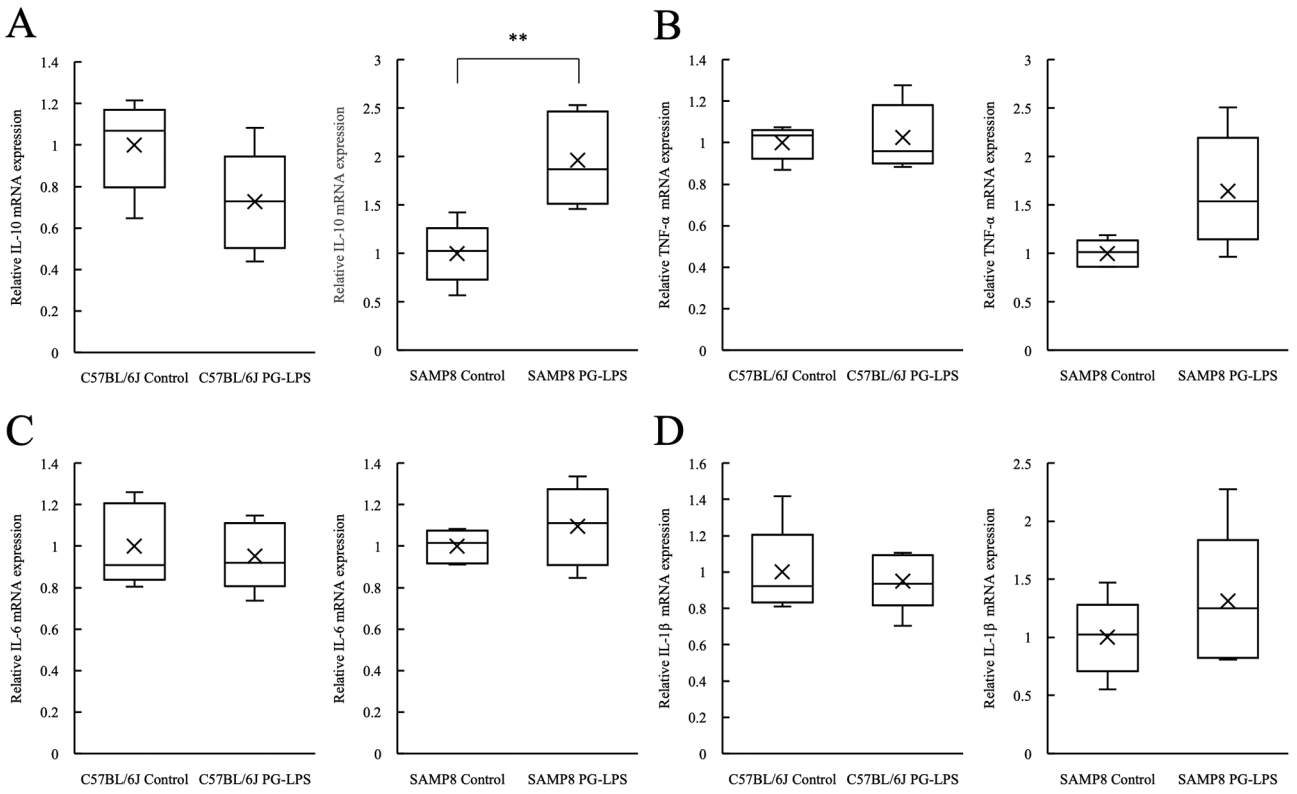

Figure 2. *mRNA levels of IL-10 (A), TNF-α (B), IL-6 (C), and IL-1β (D) in the hippocampal tissues from C57BL/6J and SAMP8 mice measured using quantitative reverse transcriptase PCR. The expression of all four mRNAs is presented relative to GADPH mRNA expression. **p<0.01 (The bar in the box plot represents median and the cross represents mean; Mann-Whitney U-test, n=5).*

visualised using a confocal microscope (Eclipse TE 2000-E; Nikon, Tokyo, Japan). Fluorescence intensity was quantified and evaluated in three random areas in the CA3 region of the hippocampus and measured using ImageJ software.

Statistical analysis. Data were compared between groups using Mann-Whitney *U*-test or Kruskal-Wallis test followed by Holm-Bonferroni method with SPSS version 26 (SPSS, Inc., Chicago, IL, USA). Results with $p<0.05$ were considered statistically significant.

Results

To determine whether PG-LPS affects the brain, the serum concentration of IL-10, a major cytokine synthesised in the central nervous system, was evaluated in PG-LPS-treated and control C57BL/6J and SAMP8 mice using enzyme-linked immunosorbent assay. The serum IL-10 concentration was significantly lower in SAMP8 mice than that in C57BL/6J mice ($p<0.05$) (Figure 1). However, in both mouse strains, the serum IL-10 concentration was significantly increased following stimulation with PG-LPS ($p<0.05$) (Figure 1). The expression of *IL-10*, *TNF-α*, *IL-6*, and *IL-1β* mRNA was observed in the brain of both C57BL/6J and SAMP8 mice (Figure 2). The expression of *IL-10* mRNA was significantly up-regulated after stimulation with PG-LPS in SAMP8 mice compared with that in the control ($p<0.01$) (Figure 2A), whereas no significant difference in the expression was observed between the PG-LPS and control groups of C57BL/6J mice (Figure 2A). There was no significant difference in *TNFα*, *IL-6*, and *IL-1β* mRNA expression between PG-LPS-treated and control C57BL/6J mice (Figure 2B, C and D).

The mRNA expression of *C1QTNF5*, *GPNMB*, *OLFML3*, *SLIT2*, *SMOC1*, and *SPON1* in the hippocampal tissues from C57BL/6J and SAMP8 mice was measured using quantitative reverse transcriptase PCR. There was no significant difference in the expression level of all six genes between PG-LPS-treated and control C57BL/6J mice (Figure 3). However, in SAMP8 mice, the mRNA expression of *C1QTNF5* and *GPNMB* was significantly higher in the PG-LPS group than that in the control group ($p<0.05$) (Figure 3A and B).

Next, we analysed the morphology of the hippocampal tissues from both C57BL/6J and SAMP8 mice using haematoxylin–eosin staining. No obvious acute inflammatory findings or changes in cell morphology, or amyloid-b

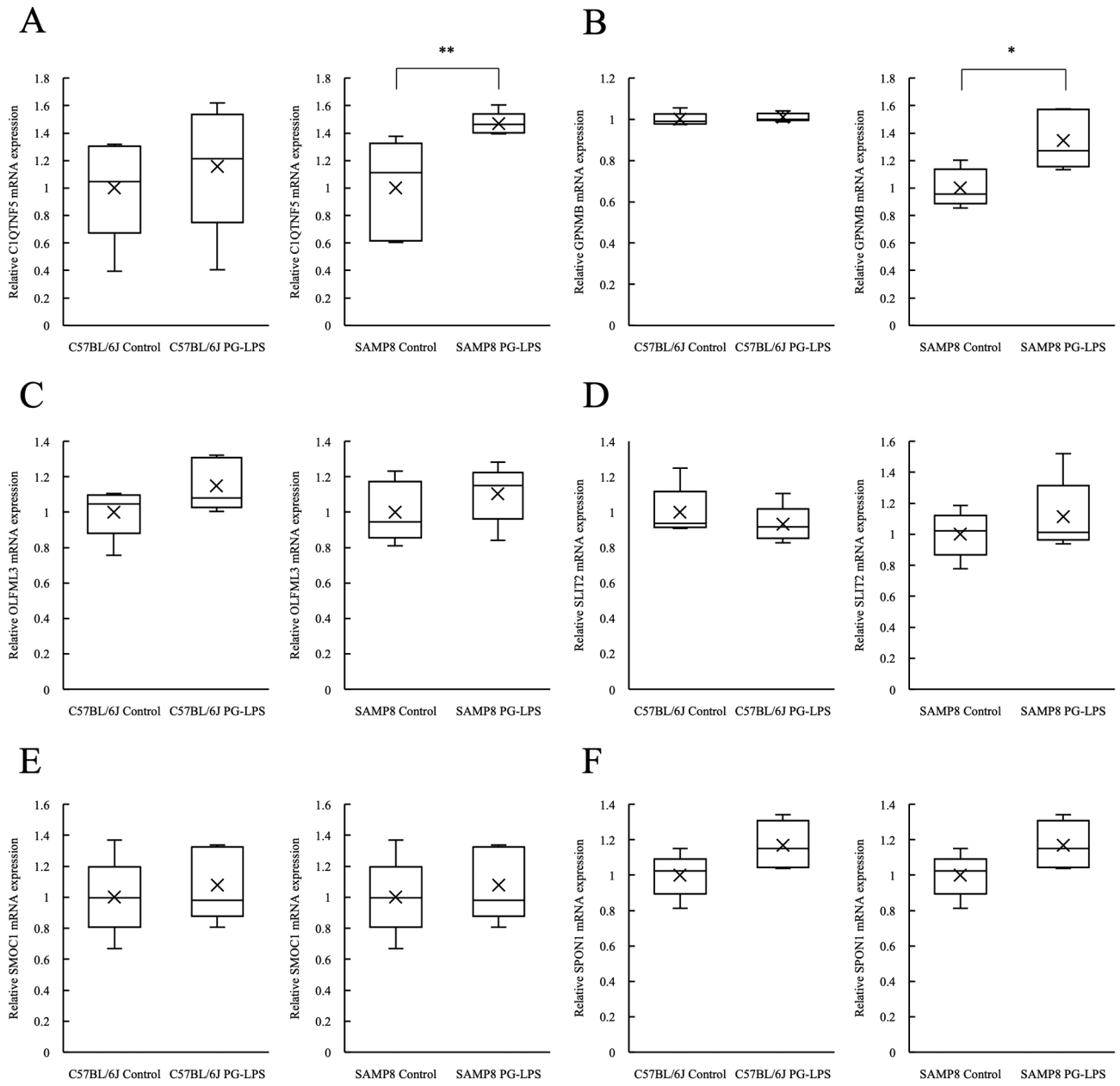

Figure 3. *mRNA levels of C1QTNF5 (A), GPNMB (B), OLFML3 (C), SLIT2 (D), SMOC1 (E), and SPON1 (F) in the hippocampal tissues from C57BL/6J and SAMP8 mice measured using quantitative reverse transcriptase PCR. The expression of all six mRNAs is presented relative to GADPH mRNA expression. *p<0.05, **p<0.01 (The bar in the box plot represents median and the cross represents mean; Mann-Whitney U-test, n=5).*

deposition were observed in the hippocampal tissues from either mouse strain (Figure 4).

The mRNA expression of neprilysin in the hippocampal tissues from C57BL/6J and SAMP8 mice was measured using quantitative reverse transcriptase PCR. There was no significant difference in neprilysin mRNA expression between PG-LPS-treated and control C57BL/6J mice (Figure 5A). However, in SAMP8 mice, neprilysin expression was significantly lower in the PG-LPS group than that in the control group (p<0.01) (Figure 5B).

Western blotting of proteins extracted from the hippocampal tissues of SAMP8 mice using a monoclonal anti-neprilysin antibody revealed a 100-kDa band (Figure 6A). The band intensity of neprilysin was significantly lower in the PG-LPS-treated group than that in the control group (p<0.01) (Figure 6B).

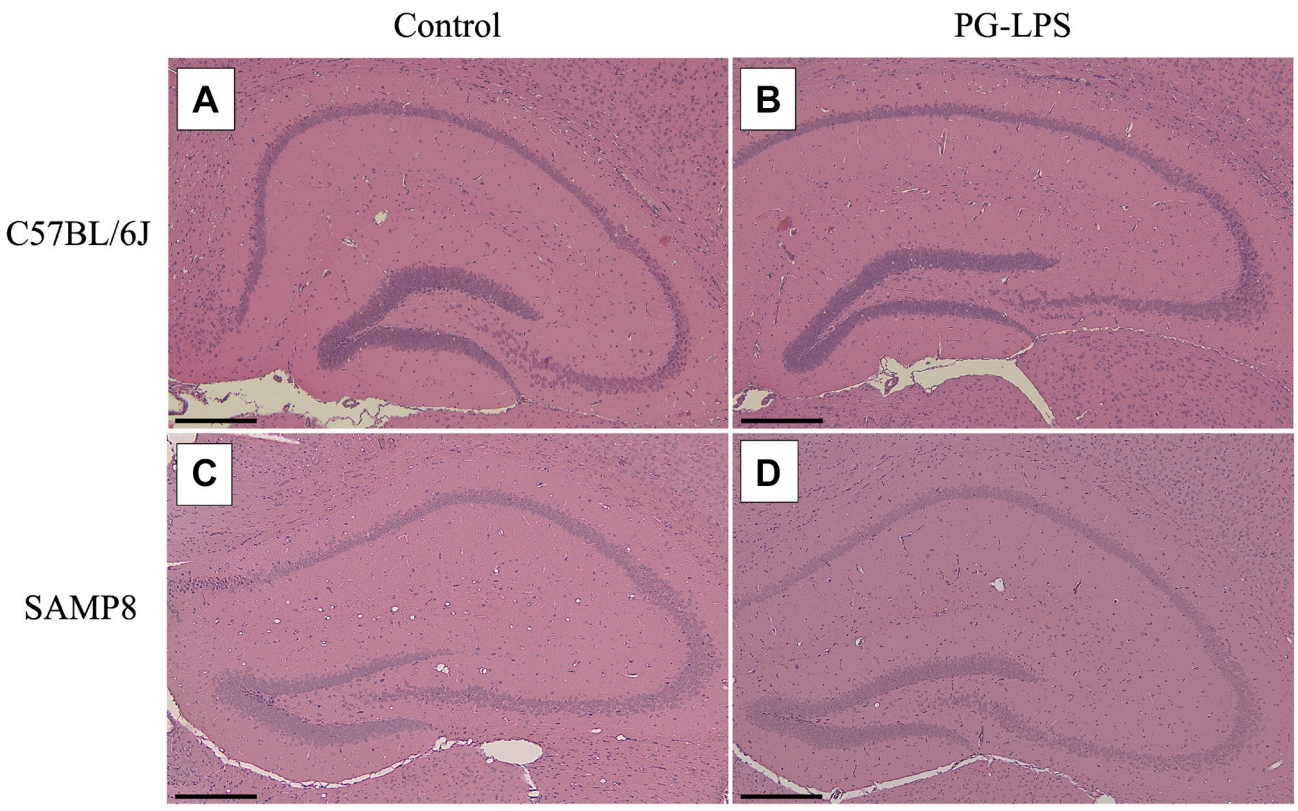

Figure 4. *Morphological analysis of the brain tissues from C57BL/6J (A, B) and SAMP8 mice (C, D). No obvious acute inflammatory findings or changes in cell morphology are observed in the hippocampal tissues from C57BL/6J or SAMP8 mice (haematoxylin–eosin staining, original magnification 100×; bar: 200 μm).*

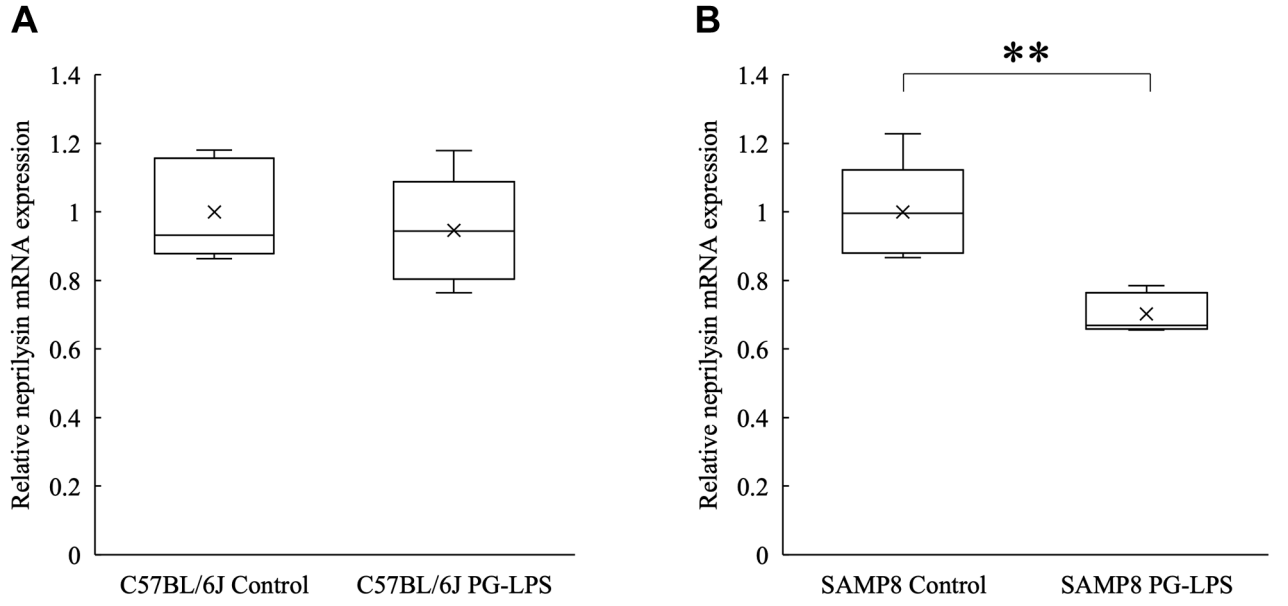

Figure 5. *Relative neprilysin mRNA level as measured using quantitative reverse transcriptase PCR in C57BL/6J mice (A) and SAMP8 mice treated with or without PG-LPS (B). Neprilysin mRNA expression is presented relative to GADPH mRNA expression. **p<0.01 (the bar in the box plot represents median and the cross represents mean; Mann-Whitney U-test, n=5).*

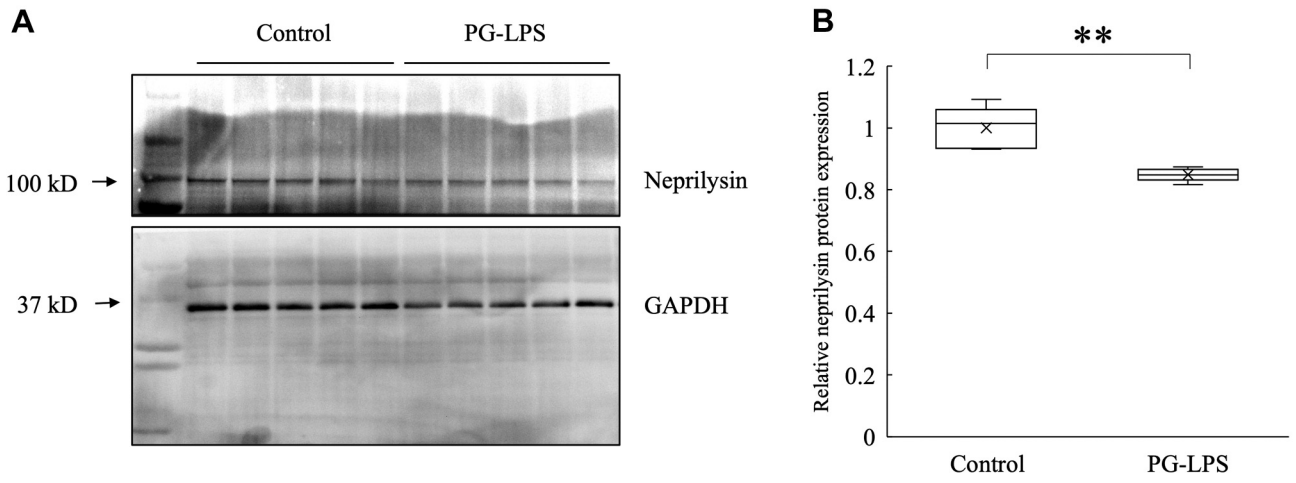

Figure 6. *Neprilysin protein levels in SAMP8 mice as measured using western blotting. (A) Western blot of neprilysin (top) and GAPDH (bottom). Neprilysin was detected as a 100-kDa band (black arrow). (B) Results of quantification of the bands. Neprilysin expression was significantly lower in the PG-LPS-treated group than that in the control group. **p<0.01 (the bar in the box plot represents median and the cross represents mean; Mann-Whitney U-test, n=5).*

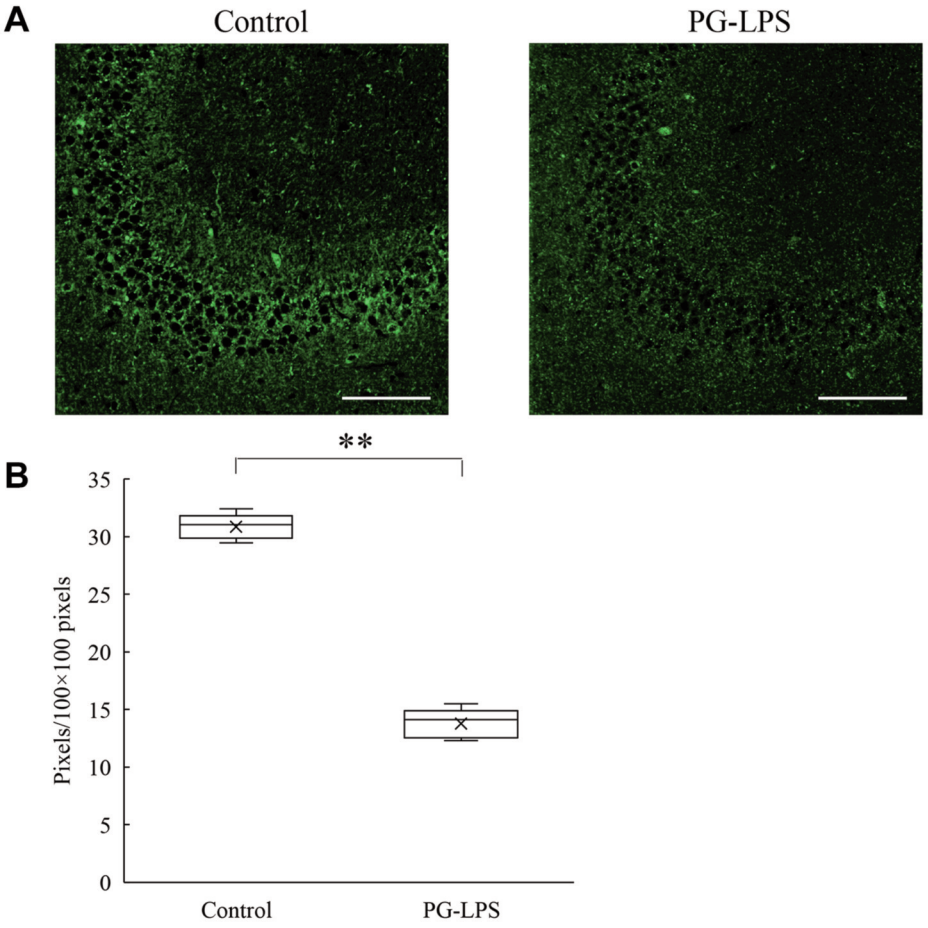

Figure 7. *Altered expression of neprilysin in the hippocampus of SAMP8 mice was evaluated using fluorescence immunohistochemical staining. (A) Immunofluorescence staining of neprilysin in the CA3 region (bar: 100 μm). The fluorescence signal was lower in the PG-LPS-treated group than that in the control group (bar: 100 μm). (B) Quantification of the data in (A). The fluorescence intensity was significantly lower in the PG-LPS-treated group than that in the control group. **p<0.01 (the bar in the box plot represents median and the cross represents mean; Mann-Whitney U-test, n=5).*

The brain tissues from SAMP8 mice were stained with an anti-neprilysin antibody. Neprilysin-positive signals were weaker for mice in the PG-LPS group than those for mice in the control group (Figure 7A). Finally, the fluorescence intensity of neprilysin in the CA3 region of the hippocampus was significantly lower in PG-LPS-treated mice than that in control mice ($p<0.01$) (Figure 7B).

Discussion

In the present study, systemic administration of PG-LPS induced the down-regulation of the amyloid-β-degrading enzyme neprilysin in SAMP8 senescence-accelerated mice, but not in non-LPS-treated mice. Although amyloid-β deposition was not observed, higher doses or longer administration of PG-LPS may lead to amyloid-β deposition. Based on our results, the down-regulation of neprilysin expression induced by *P. gingivalis* may, at least partially, be involved in increased amyloid-β deposition in elderly individuals.

Neprilysin expression did not significantly differ between PG-LPS-treated and non-treated C57BL/6J mice. The blood–brain barrier controls the movement of solutes between the blood and brain (17); hence, the blood–brain barrier may have prevented PG-LPS from penetrating the brain of C57BL/6J mice. In this study, we used 6–8-week-old mice that were stimulated with LPS for 3 months. SAMP8 mice exhibit age-related learning and memory deficit at 2 months of age (18) and signs of aging at 4 months of age (19). Two- to five-month-old SAMP8 mice have been used as Alzheimer disease models (20). Therefore, SAMP8 and C57BL/6J mice used in this study represent aged and young individuals, respectively. The blood–brain barrier is disrupted in SAMP8 mice after 3 months of age (21), possibly leading to the down-regulation of PG-LPS-stimulated neprilysin expression in these mice.

A recent study proposed novel biomarker candidates for Alzheimer's disease, including SMOC1, C1QTNF5, OLFML3, SLIT2, SPON, and GPNMB (22). As no amyloid-b deposition was found in the histological sections, we evaluated the biomarker candidates for Alzheimer's disease. Among these markers, the expression of C1QTNF5 and GPNMB was significantly higher in SAMP8 mice stimulated with PG-LPS than that in the SAMP8 controls. There were no significant changes in the expression of any of the markers between C57BL/6J mice stimulated with PG-LPS and C57BL/6J mice. These findings indicate that SAMP8 mice stimulated with PG-LPS were in the process of developing Alzheimer's disease. C1QTNF5 belonging to the C1QTNF superfamily is widely expressed in various cells, with the highest expression in adipose tissue, functions in metabolic regulation (23), and is a candidate biomarker for inflammatory chronic obstructive pulmonary diseases (24). GPNMB is a biomarker for Alzheimer's disease, and potentially activates microglia in the neuroinflammatory response (25). GPNMB promotes the polarisation of macrophages into an anti-inflammatory state, resulting in the secretion of IL-10. Increased IL-10 mRNA expression was observed in the brain of SAMP8 mice stimulated with PG-LPG, which may have been promoted by the increased expression of GPNMB.

IL-10 is an anti-inflammatory and immunosuppressive cytokine, and it modulates the inflammatory process in brain cells (26). Increased IL-10 expression lowers the brain's susceptibility to microbial infection and LPS-induced inflammation (27-29). An increased serum IL-10 concentration was observed following PG-LPS treatment in both C57BL/6J and SAMP8 mice, indicating systemic inflammation caused by PG-LPS. Increased IL-10 mRNA expression was observed in the brain of SAMP8 mice stimulated with PG-LPS, whereas no significant difference in the expression was observed between PG-LPS-stimulated and control C57BL/6J mice. PG-LPS may reach the brain cells through disrupted blood–brain barrier, leading to the increased expression of IL-10. Interestingly, decreased neprilysin mRNA expression in the brain of transgenic mice with IL-10-over-expression has been reported (30). Thus, down-regulation of neprilysin expression may have occurred because of increased levels of IL-10 in the brain.

Conclusion

We demonstrated that systemic administration of PG-LPS induced the down-regulation of neprilysin expression in senescence-accelerated mice. Down-regulation of neprilysin, an amyloid-β-degrading enzyme, may have caused increased amyloid-β deposition. Therefore, *P. gingivalis*-induced down-regulation of neprilysin expression may be involved in increased amyloid-β deposition in elderly individuals. Neprilysin shows potential as a therapeutic target for amyloid-β deposition in elderly individuals. However, we did not observe amyloid-β deposition in our experimental model. Therefore, further investigations using different experimental models are required to confirm our hypothesis.

Funding

This work was supported by the Japan Society for the Promotion of Science (JSPS) KAKENHI [grant number 17K11681].

Conflicts of Interest

The Authors have no conflicts of interest to declare in relation to this study.

Authors' Contributions

Tetsuro Morikawa: Conceptualisation, methodology, writing—original draft preparation, writing—review and editing, visualisation, supervision, project administration. Osamu Uehara:

Conceptualisation, methodology, writing—original draft preparation, writing—review and editing, visualisation, supervision, project administration, funding acquisition. Durga Paudel: Methodology, writing—original draft preparation, writing—review and editing. Koki Yoshida: Methodology, writing—review and editing, project administration, funding acquisition. Fumiya Harada: Methodology, writing—review and editing. Daichi Hiraki: Methodology, writing—review and editing. Jun Sato: Methodology, writing—review and editing. Hirofumi Matsuoka: Methodology, writing—review and editing. Yasuhiro Kuramitsu: methodology, writing—review and editing. Makoto Michikawa: Conceptualisation, methodology, writing—review and editing. Yoshihiro Abiko: Conceptualisation, methodology, writing—original draft preparation, writing—review and editing, supervision, project administration, funding acquisition. All Authors have read and approved the final version of the manuscript.

Acknowledgements

The Authors would like to thank Editage (www.editage.com) for English language editing.

References

1 Zhang H, Wei W, Zhao M, Ma L, Jiang X, Pei H, Cao Y and Li H: Interaction between Aβ and Tau in the pathogenesis of Alzheimer's disease. Int J Biol Sci *17(9)*: 2181-2192, 2021. PMID: 34239348. DOI: 10.7150/ijbs.57078

2 Steinman J, Sun HS and Feng ZP: Microvascular alterations in Alzheimer's disease. Front Cell Neurosci *14*: 618986, 2021. PMID: 33536876. DOI: 10.3389/fncel.2020.618986

3 Ballard C, Gauthier S, Corbett A, Brayne C, Aarsland D and Jones E: Alzheimer's disease. Lancet *377(9770)*: 1019-1031, 2011. PMID: 21371747. DOI: 10.1016/S0140-6736(10)61349-9

4 Wang S, Wang R, Chen L, Bennett DA, Dickson DW and Wang DS: Expression and functional profiling of neprilysin, insulin-degrading enzyme, and endothelin-converting enzyme in prospectively studied elderly and Alzheimer's brain. J Neurochem *115(1)*: 47-57, 2010. PMID: 20663017. DOI: 10.1111/j.1471-4159.2010.06899.x

5 Nalivaeva NN, Zhuravin IA and Turner AJ: Neprilysin expression and functions in development, ageing and disease. Mech Ageing Dev *192*: 111363, 2020. PMID: 32987038. DOI: 10.1016/j.mad.2020.111363

6 Iwata N, Tsubuki S, Takaki Y, Watanabe K, Sekiguchi M, Hosoki E, Kawashima-Morishima M, Lee HJ, Hama E, Sekine-Aizawa Y and Saido TC: Identification of the major Abeta1-42-degrading catabolic pathway in brain parenchyma: suppression leads to biochemical and pathological deposition. Nat Med *6(2)*: 143-150, 2000. PMID: 10655101. DOI: 10.1038/72237

7 Kim N and Lee HJ: Target enzymes considered for the treatment of Alzheimer's disease and Parkinson's disease. Biomed Res Int *2020*: 2010728, 2020. PMID: 33224974. DOI: 10.1155/2020/2010728

8 Gil-Montoya JA, Barrios R, Santana S, Sanchez-Lara I, Pardo CC, Fornieles-Rubio F, Montes J, Ramírez C, González-Moles MA and Burgos JS: Association between periodontitis and amyloid β peptide in elderly people with and without cognitive impairment. J Periodontol *88(10)*: 1051-1058, 2017. PMID: 28598287. DOI: 10.1902/jop.2017.170071

9 Kamer AR, Pirraglia E, Tsui W, Rusinek H, Vallabhajosula S, Mosconi L, Yi L, McHugh P, Craig RG, Svetcov S, Linker R, Shi C, Glodzik L, Williams S, Corby P, Saxena D and de Leon MJ: Periodontal disease associates with higher brain amyloid load in normal elderly. Neurobiol Aging *36(2)*: 627-633, 2015. PMID: 25491073. DOI: 10.1016/j.neurobiolaging.2014.10.038

10 Ding Y, Ren J, Yu H, Yu W and Zhou Y: Porphyromonas gingivalis, a periodontitis causing bacterium, induces memory impairment and age-dependent neuroinflammation in mice. Immun Ageing *15*: 6, 2018. PMID: 29422938. DOI: 10.1186/s12979-017-0110-7

11 Ishida N, Ishihara Y, Ishida K, Tada H, Funaki-Kato Y, Hagiwara M, Ferdous T, Abdullah M, Mitani A, Michikawa M and Matsushita K: Periodontitis induced by bacterial infection exacerbates features of Alzheimer's disease in transgenic mice. NPJ Aging Mech Dis *3*: 15, 2017. PMID: 29134111. DOI: 10.1038/s41514-017-0015-x

12 Zeng F, Liu Y, Huang W, Qing H, Kadowaki T, Kashiwazaki H, Ni J and Wu Z: Receptor for advanced glycation end products up-regulation in cerebral endothelial cells mediates cerebrovascular-related amyloid β accumulation after Porphyromonas gingivalis infection. J Neurochem *158(3)*: 724-736, 2021. PMID: 32441775. DOI: 10.1111/jnc.15096

13 Harada F, Uehara O, Morikawa T, Hiraki D, Onishi A, Toraya S, Adhikari BR, Takai R, Yoshida K, Sato J, Nishimura M, Chiba I, Wu CZ and Abiko Y: Effect of systemic administration of lipopolysaccharides derived from Porphyromonas gingivalis on gene expression in mice kidney. Med Mol Morphol *51(3)*: 156-165, 2018. PMID: 29388058. DOI: 10.1007/s00795-018-0181-3

14 Hiraki D, Uehara O, Kuramitsu Y, Morikawa T, Harada F, Yoshida K, Akino K, Chiba I, Asaka M and Abiko Y: P. gingivalis lipopolysaccharide stimulates the upregulated expression of the pancreatic cancer-related genes regenerating islet-derived 3 A/G in mouse pancreas. Int J Mol Sci *21(19)*: 7351, 2020. PMID: 33027970. DOI: 10.3390/ijms21197351

15 Festing MF: On determining sample size in experiments involving laboratory animals. Lab Anim *52(4)*: 341-350, 2018. PMID: 29310487. DOI: 10.1177/0023677217738268

16 Livak KJ and Schmittgen TD: Analysis of relative gene expression data using real-time quantitative PCR and the 2(-Delta Delta C(T)) Method. Methods *25(4)*: 402-408, 2001. PMID: 11846609. DOI: 10.1006/meth.2001.1262

17 Sweeney MD, Zhao Z, Montagne A, Nelson AR and Zlokovic BV: Blood-brain barrier: from physiology to disease and back. Physiol Rev *99(1)*: 21-78, 2019. PMID: 30280653. DOI: 10.1152/physrev.00050.2017

18 Akiguchi I, Pallàs M, Budka H, Akiyama H, Ueno M, Han J, Yagi H, Nishikawa T, Chiba Y, Sugiyama H, Takahashi R, Unno K, Higuchi K and Hosokawa M: SAMP8 mice as a neuropathological model of accelerated brain aging and dementia: Toshio Takeda's legacy and future directions. Neuropathology *37(4)*: 293-305, 2017. PMID: 28261874. DOI: 10.1111/neup.12373

19 Yanai S and Endo S: Early onset of behavioral alterations in senescence-accelerated mouse prone 8 (SAMP8). Behav Brain Res *308*: 187-195, 2016. PMID: 27093926. DOI: 10.1016/j.bbr.2016.04.026

20 Akbor MM, Kim J, Nomura M, Sugioka J, Kurosawa N and Isobe M: A candidate gene of Alzheimer diseases was mutated

in senescence-accelerated mouse prone (SAMP) 8 mice. Biochem Biophys Res Commun *572*: 112-117, 2021. PMID: 34364289. DOI: 10.1016/j.bbrc.2021.07.095

21 Del Valle J, Duran-Vilaregut J, Manich G, Camins A, Pallàs M, Vilaplana J and Pelegrí C: Time-course of blood-brain barrier disruption in senescence-accelerated mouse prone 8 (SAMP8) mice. Int J Dev Neurosci *27(1)*: 47-52, 2009. PMID: 18992318. DOI: 10.1016/j.ijdevneu.2008.10.002

22 Wang H, Dey KK, Chen PC, Li Y, Niu M, Cho JH, Wang X, Bai B, Jiao Y, Chepyala SR, Haroutunian V, Zhang B, Beach TG and Peng J: Integrated analysis of ultra-deep proteomes in cortex, cerebrospinal fluid and serum reveals a mitochondrial signature in Alzheimer's disease. Mol Neurodegener *15(1)*: 43, 2020. PMID: 32711556. DOI: 10.1186/s13024-020-00384-6

23 Schmid A, Kopp A, Aslanidis C, Wabitsch M, Müller M and Schäffler A: Regulation and function of C1Q/TNF-related protein-5 (CTRP-5) in the context of adipocyte biology. Exp Clin Endocrinol Diabetes *121(5)*: 310-317, 2013. PMID: 23430573. DOI: 10.1055/s-0032-1333299

24 Li D, Wu Y, Tian P, Zhang X, Wang H, Wang T, Ying B, Wang L, Shen Y and Wen F: Adipokine CTRP-5 as a potential novel inflammatory biomarker in chronic obstructive pulmonary disease. Medicine (Baltimore) *94(36)*: e1503, 2015. PMID: 26356719. DOI: 10.1097/MD.0000000000001503

25 Hüttenrauch M, Ogorek I, Klafki H, Otto M, Stadelmann C, Weggen S, Wiltfang J and Wirths O: Glycoprotein NMB: a novel Alzheimer's disease associated marker expressed in a subset of activated microglia. Acta Neuropathol Commun *6(1)*: 108, 2018. PMID: 30340518. DOI: 10.1186/s40478-018-0612-3

26 Porro C, Cianciulli A and Panaro MA: The regulatory role of IL-10 in neurodegenerative diseases. Biomolecules *10(7)*: 1017, 2020. PMID: 32659950. DOI: 10.3390/biom10071017

27 Cianciulli A, Dragone T, Calvello R, Porro C, Trotta T, Lofrumento DD and Panaro MA: IL-10 plays a pivotal role in anti-inflammatory effects of resveratrol in activated microglia cells. Int Immunopharmacol *24(2)*: 369-376, 2015. PMID: 25576658. DOI: 10.1016/j.intimp.2014.12.035

28 Gutierrez-Murgas YM, Skar G, Ramirez D, Beaver M and Snowden JN: IL-10 plays an important role in the control of inflammation but not in the bacterial burden in S. epidermidis CNS catheter infection. J Neuroinflammation *13(1)*: 271, 2016. PMID: 27737696. DOI: 10.1186/s12974-016-0741-1

29 Martin NM and Griffin DE: Interleukin-10 modulation of virus clearance and disease in mice with alphaviral encephalomyelitis. J Virol *92(6)*: e01517-17, 2018. PMID: 29263262. DOI: 10.1128/JVI.01517-17

30 Chakrabarty P, Li A, Ceballos-Diaz C, Eddy JA, Funk CC, Moore B, DiNunno N, Rosario AM, Cruz PE, Verbeeck C, Sacino A, Nix S, Janus C, Price ND, Das P and Golde TE: IL-10 alters immunoproteostasis in APP mice, increasing plaque burden and worsening cognitive behavior. Neuron *85(3)*: 519-533, 2015. PMID: 25619653. DOI: 10.1016/j.neuron.2014.11.020

Received November 16, 2022
Revised November 29, 2022
Accepted November 30, 2022